MAPPING DUNE VEGETATION USING IMAGING SPECTROSCOPY FOR AMELAND, THE NETHERLANDS

Arjan J.H. Meddens[1], Lammert Kooistra[1], Anne M. Schmidt[2], Han F. van Dobben[3], Michael E. Schaepman[1] and Pieter A. Slim[3]*

1. Wageningen University, Department Environmental Sciences, Laboratory of Geo-information Science and Remote Sensing, Wageningen, The Netherlands, Arjan.meddens@gmail.com; Lammert.Kooistra@wur.nl; Michael.Schaepman@wur.nl
2. Alterra, Centre Geo-information, Wageningen, The Netherlands, Anne.Schmidt@wur.nl
3. Alterra, Centre Landscape, Wageningen, The Netherlands, Han.vandobben@wur.nl; Pieter.slim@wur.nl

ABSTRACT

The possibility to map vegetation types using imaging spectroscopy in a coastal area was investigated. This landscape is under the influence of changing salt water inundation regimes, resulting in a heterogeneous composition of the vegetation structure. The species composition in the area of interest was described by means of vegetation relevees. A vegetation typology used in former studies was adopted to perform the hyperspectral image classification. The vegetation classes to be derived from image classification were identified as wet brackish dune valleys, dune shrub, beach grass dunes (white dunes) and grassy dunes (grey dunes). The commonly used maximum likelihood classification (MLHC) was used to classify a hyperspectral image, acquired by the AHS sensor. A new method of data reduction was explored, namely the redundancy analysis (RDA) in the software package CANOCO. The RDA was used to reduce the spectral data dimensionality and to determine which bands of the hyperspectral imagery had the most predictive power to distinguish the selected vegetation types. The band selection from the vegetation observation dataset was used to perform a MLHC and was then compared to a MLHC using a PCA transformation. A maximum classification accuracy of 64.8% was found when MLHC was employed for differentiation of the four vegetation types. The influence of soil background was an important source of variation in the hyperspectral dataset making separation of the different vegetation classes more difficult. Mapping and monitoring dune vegetation using hyperspectral imagery could further be enhanced when ancillary data (e.g. digital elevation models or multi-temporal imagery) is included in the analyses.

Keywords: Remote sensing, imaging spectroscopy, vegetation mapping, dune vegetation.

INTRODUCTION

Vegetation monitoring is required to understand the dynamics of the biodiversity of a certain area and is often a baseline for ecological research. To be able to map or monitor vegetation, plant sociological groups are classified into vegetation types. Local scale vegetation is clustered according to the similarity of plant species composition often followed by a vegetation typology. In order to classify and investigate plant species composition efficiently the two-way classification program, TWINSPAN (i) and the multivariate ordination program, CANOCO (ii) are generally used. The vegetation classification system, which is widely used across Europe (iii), and increasingly elsewhere, is the Braun-Blanquet system. This system describes plant assemblages at different hierarchical levels namely, class order, alliance and association. Various methods exist to derive vegetation maps from vegetation observations, these include: Arial Photo Interpretation (API) (iv) interpolation on the basis of (permanent) vegetation quadrats (e.g. kriging, (v)), simple interpolation using Thiessen polygons (vi), or even in field vegetation border determination on the basis of field maps.

Figure 1: The location and border of the study site on the Wadden island Ameland in the North of the Netherlands. (Source: NLR Remote Sensing Department)

Lately, depending on the purpose and scale, new methods of vegetation mapping and monitoring have been proposed using remote sensing techniques. Janssen *et al.* (iv) identified possibilities and problems using multispectral digital image manipulation. Schmidt & Skidmore (vii) found that hyperspectral sensors can improve the mapping of plant species (floristic composition of the vegetation) on salt marshes on the Wadden island Schiermonikoog. Thomson *et al.* (viii) made vegetation maps of dune vegetation with an approximate 70% accuracy with ground based data in the Westerschelde.

The possibilities of the use of recent remote sensing techniques in vegetation mapping and monitoring are: (1) objective classification, as opposed to manual aerial photo interpretation (API) (iv and ix); (2) a quick and repeatable method to monitor change of spectral separable vegetation units (x) and (3) the possibility to extract information of vegetation over a full coverage in the region of interest (xi). Drawbacks are that: (1) a standard approach is currently lacking (xii) and (2) the atmospheric illumination effects and plant phenology vary over time, complicating comparison between different images (xiii).

The research for this study is done to evaluate possible improvements for making full coverage vegetation maps for dune vegetation on Ameland, the Netherlands. Ameland is one of the Dutch “wadden” islands and for a large part nature area (xiv) which is included in Natura 2000 program. In 2001 and 2004 field studies (v) were conducted to evaluate vegetation type transitions due to gas extraction and the subsequent soil subsidence. Vegetation sampling is an extensive and expensive part of that investigation and commissioners are interested in less expensive, objective and repeatable methods to achieve full coverage vegetation maps to map and monitor vegetation change. Since 1986, the effect of the gas extractions and the subsequent soil subsidence on vegetation has been monitored to secure a possible decline of biodiversity in the protected habitat of Ameland. Future vegetation sampling and mapping could be more effective (e.g. improved accuracy, objectivity or repeatability) if hyperspectral remote sensing is included in the sampling method.

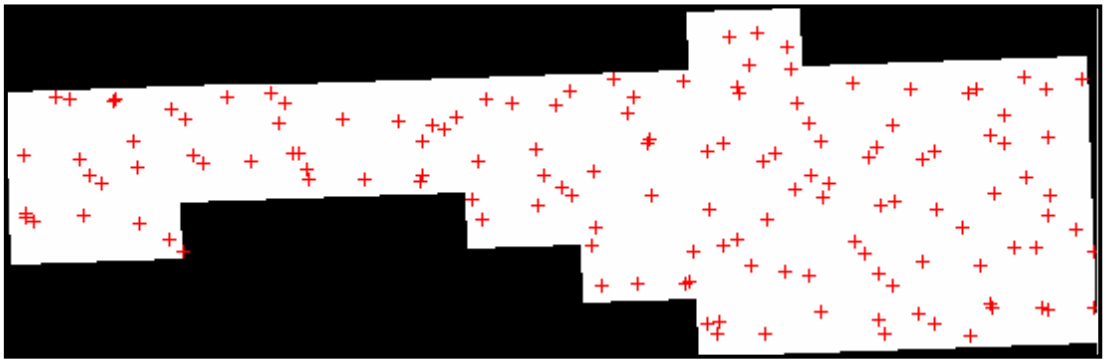

Figure 2: The "unaligned systematic sampling" points of the vegetation dataset.

METHODS

Study site

The study site is situated on the Eastern part of Ameland. Ameland is one of the Dutch barrier islands in the Wadden, the northern part of the Netherlands (figure 1). The borders of the study area were taken from the study of Slim *et al.* (v). The size of the study site is approximately 70.2 ha. The present vegetation consists of almost bare dune sand, dune grass, dune shrubs and on the lower parts, salt marches. Vegetation in the lower parts of the area on the south eastern shore is regularly inundated. These vegetation associations show clear transitions, the vegetation is mostly depended on the height in the field and the resulting salt water influence. Yearly sedimentation and erosion is taking place causing a yearly shift of the vegetation types. The vegetation on Ameland is well described by ecological experts and botanists (e.g. (xiv)). The vegetation is characterised by rare vegetation associations caused by the influence of salt water and is of ecological importance to the Wadden area. The eastern part of Ameland is part of the nature protection program Natura 2000.

Vegetation sampling

In August 2004, 140 vegetation relevees were described as part of a soil subsidence investigation and the possible effects on vegetation (v). The vegetation relevees are circular with area of 4m² (r = 1.13m) and all vascular plants and mosses were identified and their coverage estimated. Five different vegetation types were described to evaluate the effect of soil subsidence on the vegetation (Table 1, A – E). These vegetation types are described in Slim *et al* (2005). In order to make a full coverage vegetation map using (universal indicator) kriging they reduced the number of vegetation types to four clearly distinctive classes, including: (B) Wet and brackish valleys, (C) Rough and shrubby dunes, (D) Beach grass dunes (seaside) and (E) Grassy dunes. Vegetation type B is characterized as wet brackish dune valleys (salt marsh), the species with high coverage in this vegetation type are Juncus *gerardi* L. and *Potentilla anserina* L. Vegetation type B is found on the lowest parts of the research site and is influenced by saltwater. Vegetation type C is characterized as dune shrub, the species with high coverage species in this vegetation type are *Salix repens* L., *Calamagrostis epigejos* L., *Hippophae rhamnoides* L., and *Urtica dioica* L. Vegetation type C has a high vegetation cover and is characterized by a high percentage of shrubs in the vegetation. Vegetation type D also known as white dunes is located along the seaside and characterized by dune grass with an open structure. The species with high coverage species in this vegetation type are *Ammophila arenaria* L., and *Carex arenaria* L. Vegetation type E is characterized as grey dunes, the species with high coverage in this vegetation type is *Hypnum cupressiforme* s.l. species (moss). Vegetation type E has a more closed and grassy herb layer.

Table 1: Vegetation types and corresponding vegetation associations (source Slim et al. (v)).

Type	Name	Corresponding vegetation association
A	Barren dune foot	*Agropyro-Honckenyion peploidis*
B11 & B12 B21 & B22	Wet, brackish dune valleys Wet, brackish dune valleys (drier)	*Lolio-Petentillion anserinae, Amerion maritimae & Saginion maritimae*
C1 C2	Dune shrub Dune shrub (wetter)	*Salicion cinereae, Berberidion vulgaris & other shrubby vegetation*
D	White dunes (seaside)	*Ammophilion arenariae, Ammophilion arenariae-Carex arenaria [Ammophophiletea/ Koelerio-Corynephoretea], Tortulo-Koelerion & Polygalo-Koelerion*
E	Grey dunes	*Tortulo-Koelerion, Polygalo- Koelerion, Calamagrostis epigejos-[Cladonio-Koelerietalia], Berberidion vulgaris*

The placement of the relevees locations was done according to a sample strategy called “unaligned systematic sampling” described by Oude Voshaar (xv) (figure 2). The sample strategy is based on the placement of a raster of regular squares across the investigated research site and starts with assigning a sample location to the first square in the upper left corner with a random X and Y coordinate. Thereafter, the sampling location of each square in the upper row gets the same X coordinate but a new randomly chosen Y coordinate. On the second row the sample location of the first square gets a new random X coordinate and the Y coordinate of the square above is maintained. The rest of the squares in the second row then get the same new X coordinate of the first square and the same Y coordinate of the square above. This is repeated on the subsequent rows till every sample locations in all squares have an X and Y coordinate. The above described sample strategy was repeated two times assigning two times 70 locations (in total 140 points) to the research site. In this way the locations have a representative dispersion over the research site. The X and Y coordinates of the placed locations were precisely geo-referenced in the Dutch RD coordinate system using RTK-DGPS.

Hyperspectral imagery

In 2005 on the 19th of June an airplane with the Airborne Hyperspectral Scanner (AHS-160) sensor conducted a flight over Eastern Ameland and acquired a hyperspectral image of the research site. The pre-processing of the AHS-160 image included a geo-correction and an atmospheric correction. This image was prepared by VITO (xvi) in Belgium and has a spatial resolution of 3.5 by 3.5 meter. VITO encountered some problems with the atmospheric correction of the MIR region of the AHS image due to irregular calibration of the sensor. The thermal bands have been acquired but were not used in this study. In table 2 the spectral bands of the AHS sensor are shown.

Table 2: AHS-160 spectral bands used for the hyperspectral data acquisition over Ameland.

Spectral region	Wavelength interval (µm)	Nr of bands
Visible/NIR[1]	0.45 - 1.05	20
Mid IR[2]	1.6 (one broad band)	1
Mid IR[2]	2 - 2.5	42

[1]Near Infra Red, [2]Infra Red.

Although, the vegetation relevees were taken a year before the time of the image acquisition, the dataset is used as the ground truth dataset because of the lack of a representative dataset at the time of the image acquisition in 2005. The changes are assumed to be fairly low. Slim *et al.* (v) reported a 14.3% change of one vegetation type into another vegetation type on the 70 locations, over three years, giving a predicted vegetation change of 4.8% over one year. This percentage was assumed to be small enough to make use of this dataset as ground truth data.

The precisely georeferenced locations of the vegetation dataset of 2004 were transformed from the Dutch RD coordinate system to UTM WGS `84 coordinates (31W) and the locations were stored in a vector file. Comparison of the vegetation relevees and reflective response recorded by the AHS sensor includes a spatial resolution difference of 4m² (vegetation relevees) to 12.25m² (pixel size AHS).

Image classification

Maximum likelihood classification (MLHC) is a straight forward and common method for classification of remote sensing images (xvii). In MLH classification, the spectral values of a pixel are classified according to the maximum likelihood for a corresponding class. Under the assumption of normality, the distribution of a category response pattern can completely be described by the mean vector and the covariance matrix (xviii). Based on these statistical parameters, we may compute the statistical probability of a given pixel value being a member of a particular class. To optimize the MLH classification, data reduction is often necessary, especially in hyperspectral data where the available number of bands exceeds the optimum number of bands for classification (xix). The limited band usage is because of two reasons; (1) more bands results in a higher uncertainty of the backwards prediction and (2) in order to obtain accurate values (to calculate the covariance) of the training set the number of pixels should be higher then the number of bands. In order to objectively obtain a limited number of bands a multivariate analysis was performed, where the species composition was explained by the spectral response. Canoco (ii) is a multivariate analyses ordination software program. The ordination method maximizes the part of the variation in species composition that can be expressed as linear combinations of predictor variables in this case reflectance (xx). The image pixel information for the sites of the observed vegetation was included as predictor variables. Because the response variables were assumed to be linear, the method of Redundancy Analyses (RDA) was chosen. A RDA ordination was performed on the on the 2004 vegetation observation data and their image spectra corresponding to relevee location in the image. All usable AHS bands (21 bands) were included as environmental variables. From the 21 bands, a forward selection was done to include the bands with the most predictive power. The criteria used were F-value > 2; p-estimate < 0.05. From the 2004 spectra twelve bands were selected using these criteria. The MLHC was performed and the accuracies were calculated. To compare the RDA band selection with other variable reduction methods, the MLHC was performed on the PCA transformed image and the accuracy was determined.

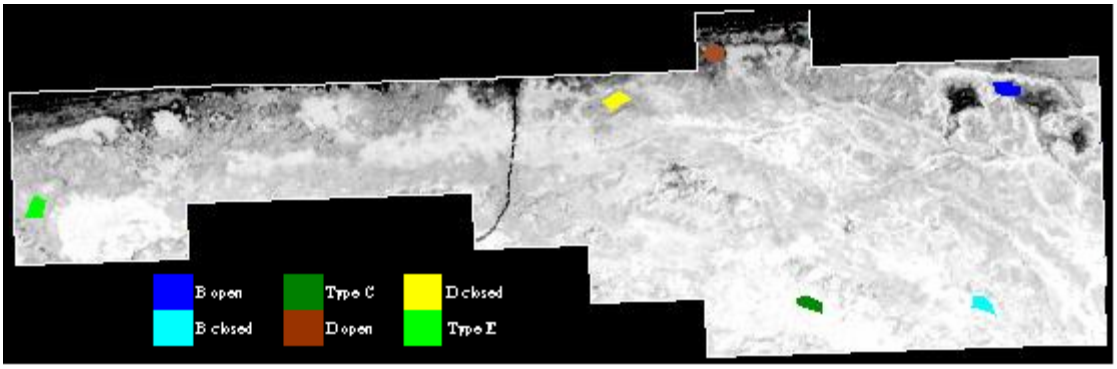

Figure 3: NDVI image and the selected trainings areas for the MLH classification for the Ameland study area. Areas with a white color are indicative for a high NDVI value.

Trainingset

The trainingset was determined from known locations in the field and with help of the kriged map in Slim *et al.* (v). In order to obtain the trainingset of the MLHC, the NDVI image of the study area (figure 3) was also investigated. Six sites with homogeneous vegetation types, of approximately 70 pixels for each training class were manually selected. Vegetation type B and D have a great variability in soil influence and for the trainingset an open and a closed type was appointed. The NDVI image indicates where the vegetation reflectance dominates the spectra (white) and where the spectra have more soil influence (black) (figure 3). The upper part of the image has great influence of dune sand, which is mainly indicative for vegetation type D. On the right top of the image a different soil dominated feature (darker and wetter soil) can be seen which is related to vegetation type B and has a different reflectance. Both soil influenced (white sand and wetter darker soil) vegetation types are incorporated as extra class in the vegetation MLHC. This results in a total of six classes for the MLHC trainingset.

Accuracy assessment

The plot locations were used to calculate the confusion matrices and kappa statistic. Two confusion matrices are obtained by the MLH classification, namely for the RDA band selection and the PCA transformed data. The confusion matrix is the most common method of accuracy determination of an image classification in remote sensing (xxi). The confusion matrix is a square assortment of numbers defined in rows and columns that represent the number of sample units (i.e. pixels, clusters of pixels or polygons) assigned to a particular category relative to the actual category as confirmed on the ground. Together with the confusion matrix and the overall accuracy, the Kappa statistic was calculated. The Kappa statistic also gives a measure of accuracy and takes into account the probability of randomly assigning correct classes to pixels. The Kappa coefficient is calculated as follows:

$$\hat{K} = \frac{Overall\_classification\_accuracy - Expected\_classification\_accuracy}{1 - Expected\_classification\_accuracy} \qquad \text{(eq.1)}$$

The Kappa statistic (xxii) is a generally accepted accuracy measurement and serves as a more rigorous estimate of accuracy considering agreement that may be expected to occur by changes. Fleiss (xviii) suggested an ordinal Kappa scale from “poor” (<0.40), “fair” (0.4-0.75) to “excellent” (>0.75).

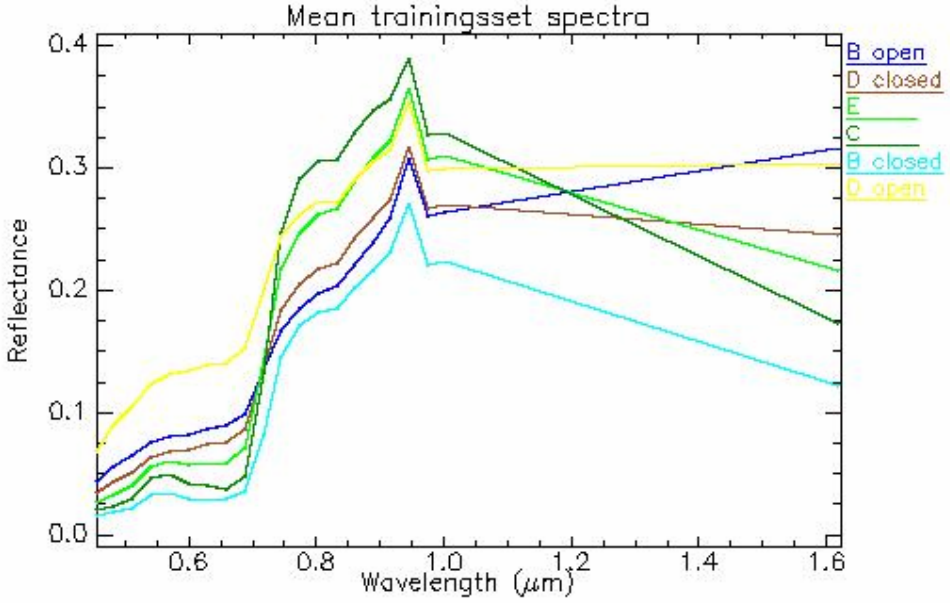

Figure 4: The averaged spectra of the manual selected trainingset derived from the AHS image.

RESULTS

In figure 4 the mean spectra of the trainingset are shown. The spectra of B open and B closed as well as D open and D closed are quite distinct and showing the need for separation into an open and closed vegetation type. When validation was performed the classes of B open and B closed and of D open, D closed were merged into one vegetation type B class and one vegetation type D class.

In figure 5 the RDA bi-plots of the species the vegetation dataset and their associated spectral band values are shown. The bands selection was done according to an F-value of 2 or higher and a predicted α of 0.05 or lower. The classification of the RDA dimension reduction was performed using the twelve selected bands form the vegetation observation locations. To evaluate the performance of band selection a comparison was made with PCA transformation/data reduction was performed to generate a MLH classification from the PCA bands. The first four PCA bands were chosen after investigating the eigenvalues plot of the PCA transformation.

The species *Potentillia ansenaria* L. and *Juncus gerardi* L. are indicative for vegetation type B, species *Salix repens* L., *Hippophae rhamnoides* L. and *Calamagrostis epigejos* L. indicative for vegetation type C, species *Ammophila arenaria* L. and *Carex arenaria* L. indicative for vegetation type D and *Hypnum cupressiforme* s.l. species (moss) indicative for vegetation type E. *Festuca rubra* L. is the only species which is present in vegetation type C, D and E and could thus cause difficulties because of similar reflective response over all three vegetation types.

The obtained classification accuracy results are 64.7% using RDA data reduction and 64.8% using PCA data reduction. The confusion matrices are show in table 3. In figure 6 the classified image of the RDA selected bands from the vegetation observations is shown. Vegetation type B had the lowest accuracy in all performed classifications and was often misclassified as vegetation type C. Vegetation types D and E had overall the highest accuracies. The classification with the RDA data reduction yielded similar accuracies then the classification with PCA.

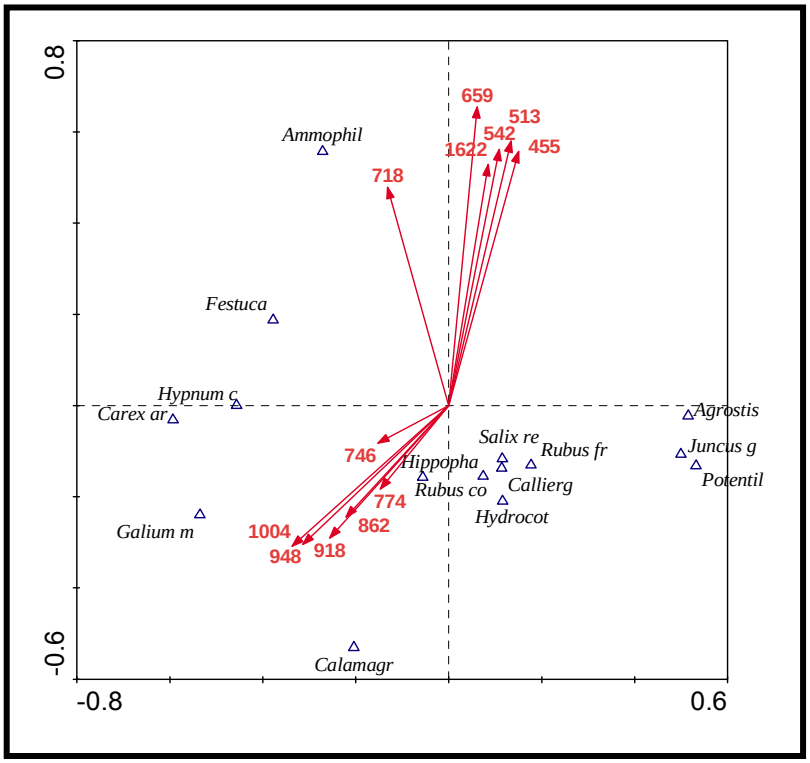

Figure 5: Biplot of the RDA of the 2004 vegetation relevees, with the twelve selected bands as predictor variables. (Forward selection: F-value > 2, p < 0.05).

DISCUSSION AND CONCLUSIONS

Figure 6 shows the classified image for the six classes using the twelve RDA selected bands. The mapped vegetation patterns correspond to the actual field situation, although vegetation type B is underestimated whereas vegetation type C is somewhat overestimated (Table 3). In addition, a slight misclassification between both the soil influenced classes (open B and open D) can be detected.

MLH classification is a widely used method and can be used for both multi- and hyperspectral imagery. When using MLH classification for hyperspectral data analyses, it is important to reduce the data dimensionality (xix). Common methods for data reduction are PCA (xviii) and Minimum noise fraction (MNF) (xxiii). In this study a method used in ecological analyses, RDA was used to objectively reduce the number of bands (with the F-value and α) and compared to the PCA data reduction method (commonly used for the MLH classification). The chosen bands from the RDA maximized the variation of returned spectra (pixels) of the locations of the plant observations in the field (figure 5) for a limited number of bands.

Table 3: Confusion matrix of the MLHC using the selected twelve spectral bands.

Vegetation Type PCA	Type B (%)	Type C (%)	Type D (%)	Type E (%)	Producer accuracy (good classified pixel/all pixels)
Type B	50.0	4.8	9.4	0	50% (12/24)
Type C	37.5	56.1	0	11.9	56.1% (23/41)
Type D	8.3	4.9	84.4	21.4	84.4% (27/32)
Type E	4.2	34.2	6.2	66.7	66.7% (28/42)
Users accuracy (good classified pixel/all pixels)	70.6 (12/17)	62.2 (23/37)	67.5 (27/40)	62.2 (28/45)	Overall accuracy = 64.8% Kappa statistic = 0.52
Vegetation Type RDA	Type B (%)	Type C (%)	Type D (%)	Type E (%)	Producer accuracy (good classified pixel/all pixels)
Type B	45.8	0	0	0	45.8%(11/24)
Type C	37.5	53.7	3.1	16.7	53.7% (22/41)
Type D	8.3	12.2	93.8	19.1	93.8% (30/32)
Type E	8.3	34.2	3.1	64.3	64.3% (27/42)
Users accuracy (good classified pixel/all pixels)	100% (11/11)	56.4% (22/39)	66.7% (30/45)	61.4% (27/44)	Overall accuracy = 64.7% Kappa statistic = 0.52

The data reduction of the MLH classification using RDA (redundancy analyses) of the software package CANOCO compared to the commonly used PCA data reduction yielded similar classification accuracy (Table 3). The RDA analyses can improve objective band selection and explains spectral response for specific species composition, excluding the variance caused by other reflectance (e.g., soil) in the imagery. The RDA method as new method for reduction of data dimensionality is also able to select bands which directly explain the spectral response of the species composition. The bands which are selected have the most variance in vegetation reflectance and are most distinctive in feature plot space and in addition, RDA also minimizes the double information of the spectral response (e.g. high correlation between bands). Future analyses on multi-temporal images could employ the same set of bands which can be selected from an objective method and which directly explains the difference in vegetation spectral response rather then making use of “image dependent” PCA transformations.

The RDA selected bands correspond to specific vegetative reflectance and absorption features, hereafter described. The bands: 455, 484 and 513nm are associated with plant pigment absorption maxima of Chlorophyll b, α-Carotene and β-Carotene. Band 542nm is associated with green light,

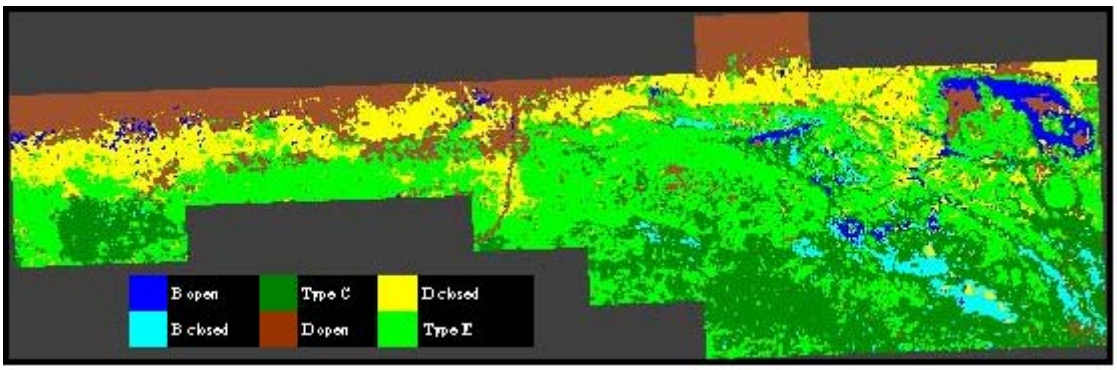

Figure 6: MLH classified image using the selected twelve RDA selected bands for the Ameland study area.

here vegetation has a slight increased reflective response. Band 659nm corresponds to a pigment absorption maximum of Chlorophyll b and is located at the begin of the red-edge, bands 718, 746 and 774 are sensitive for the red-edge region. Bands 804, 918, 948, 1004 and 1622 are in the NIR region and give increased reflectance with increased vegetation structure.

Vegetation spectral reflectance in the research site is highly influenced by the soil (figure 3). The degree of vegetation cover in relation to the exposure of the soil is the predominant factor influencing which classes can be distinguished (viii). The influence of soil in the spectra was an important source of variation in the dataset. This caused difficulties when the vegetation was classified solely on vegetation specific reflectance for the MLH classification. In order to obtain an accurate classification with the MLHC, the vegetation classes were split into an open and a closed vegetation variant in two of the four vegetation classes (Vegetation type B and D).

Although the appointing of classes to locations is more objective using remote sensing, the choice of trainingset still remains subjective. Experts still have to appoint representative vegetation classes to be able to make use of training areas. The usage of spectral libraries with endmembers (e.g. pure reflective response of one vegetation type) established outside of the image is a possibility to improve the objectivity. However the difference in spatial resolution and the difference in atmospheric correction are the major causes of failing to establish a spectral library from the field spectrometer measurements.

The 2004 dataset had a time lack of one year compared to the acquisition of the hyperspectral imagery. This could have caused vegetation transitions in the year in-between the field sampling and the image acquisition, which cannot be traced. However, the changes were assumed to be relatively small (Slim, pers comm.). The dataset still proved to be useful for accuracy determination and the unaligned systematic sample strategy gave a representative distribution of observation points over the research site.

The validation of the dataset was done by vegetation classes observed in the field, these observations had a sampled area of 4m² .The difference in the sampled area of the vegetation observations (4m²) and the pixel sizes (12.25m²) could include that pixels have more than one vegetation type. In this study the classified vegetation type of the vegetation observation datasets were used as ground truth for the whole image pixels. In future field data collection for image validation, the pixel sizes should be taken into account in order to improve the estimation of the accuracy of the classification.

Next to the difficulties of the sample strategy, there were some difficulties with the calibration of the AHS sensor in the MIR region (2000nm to 2500nm). Therefore only 21 bands in the visible and in the NIR region where used. Some vegetation types could be more accurately separated by classification methods when the MIR bands where included in the analyses, therefore the obtained accuracy could have been slightly lower then when the MIR bands were included in the analyses.

REFERENCES

i Hill M O, 1979. TWINSPAN – a FORTRAN program for arranging multivariate data in an ordered two-way table by classification of the individuals and attributes. Ecology and Systematics. Cornell University, Ithaca, New York..

ii Ter Braak C J F, 1988. CANOCO - a FORTRAN program for canonical community ordination by (partial) (detrended) (canonical) correspondence analysis, principal components analysis and redundancy analysis (version 2.1). Technical Report LWA-88-02, GLW, Wageningen.

iii Schaminée J H J, P W F M Hommel, A H F Stortelder, E J Weeda & V Westhoff, 1995. De Vegetatie van Nederland, Opulus Press, Uppsala/Leiden. Vol 1-5.

iv Janssen J A M, E H Kloosterman, J van den Bergs & L M L Zonneveld, 1995. Het Ameland schalenproject; de mogelijkheden van remote sensing technieken voor vegetatiemonitoring ten behoeve van natuurbeheer. BeleidsCommissie Remote Sensing (BCRS), the Netherlands.

v Slim P A, G B M Heuvelink, H Kuipers, G M Dirkse & H F Dobben van, 2005. Vegetatiemonitoring en geostatistische vegetatiekartering duinvalleien Ameland-Oost. In: Monitoring effecten van bodemdaling op Ameland-Oost., Beleidscommissie Monitoring Bodemdaling Ameland.

vi Sanders M E, G M Dirkse, P A Slim, 2002. Vegetatiekartering en monitoring van twee graslanden in het Lauwersmeer gebied in 1998 & 2002, Alterra report, 1136, Wageningen, The Netherlands.

vii Schmidt K S & Skidmore A K, 2003. Spectral discrimination of vegetation types in a coastal wetland. Remote Sensing of Environment 85:92-108.

viii Thomson A G, A Huiskes, R Cox, R A Wadsworth & L A Boorman, 2004. Short-term vegetation succession and erosion identified by airborne remote sensing of Westerschelde salt marshes, The Netherlands. International Journal of Remote Sensing 25(20):4151-4176.

ix Janssen J A M & B van Gennip, 2000. De oude grenzen methode. Landschap 17(3/4):177-185.

x Kokaly R F, D G Despain, R N Clark & K E Livo, 2003. Mapping vegetation in Yellowstone National Park using spectral analyses of AVRIS data. Remote Sensing of Environment 84:437-456.

xi Williams A P & E J Hunt jr., 2002. Estimation of leafy spurge cover form hyperspectral imagery using mixture tuned matched filtering. Remote Sensing of Environment 82:446-456.

xii Silvestri S, M Marani, J Settle, F Benvenuto & A Marani, 2002. Salt marsh radiometry data analyses and scaling. Remote Sensing of Envirnment 80:473-482.

xiii Schmid T, M Koch & J Gumuzzio, 2005. Multisensor approach to determine changes of wetland characteristics in semiarid environments (central Spain). IEEE Transactions on Geoscience and Remote Sensing 43(11): 2516-2525.

xiv Westhoff, V & M F van Oosten, 1991. De plantengroei van de waddeneilenden. Stichting van de Koningklijke Nederlandse Natuurhistorische Vereniging, Utrecht, The Netherlands.

xv Oude Voshaar JH, 1981. Steekproefmethoden in het onderzoek naar de verspreiding van perceelsvormen: oppervlakteschatting van mozaieken via puntsteekproeven. IWIS-TNO, Wageningen, the Netherlands.

xvi VITO report, 2005. Processing and archiving facility for airborne remote sensing: software system validation report, AHS160 Campaign 2005. Vito Center of Remote Sensing & Earth Observation Processes, Belgium.

xvii Lillesand T M & R W Kiefer, 2000. Remote sensing and image interpretation (4th ed.). John Wiley & Sons Inc., New York, USA.

xviii Fleiss J L, 1981. Statistical methods for rates and proportions. 2nd edition. Wiley, New York, p. 38-46.

xix Verrelst J, 2004. Adopting plant community data for floodplain vegetation mapping using an image fusion of CASI and LiDAR data. Thesis report GRS-2004-40, Wageningen University, the Netherlands.

xx Schmidtlein S & J Sassin, 2004. Mapping continuous floristic gradients in grasslands using hyperspectral imagery. Remote Sensing of Environment 92:126-138.

xxi Congalton R G, 1991. A review of assessing the accuracy of classifications of remotely sensed data. Remote Sensing of Environment 37:35-46.

xxii Cohen, J (1960). A coefficient of agreement for nominal scales. *Educational and Psychological Measurement*, 20:37–46.

xxiii Green A A, Berman M, P Switser & D M Craig, 1988. A transformation for ordering multispectral data in terms of image quality with implications for noise removal. IEEE Transactions on Geoscience and Remote Sensing 26(1):65-74.